

CHEMISTRY

A European Journal

A Journal of



Accepted Article

Title: Self-Assembly of Cyclohelicate [M3L3] Triangles over [M4L4] Squares, despite near Linear bis-terdentate L and Octahedral M

Authors: Sally Brooker, Ross Hogue, Sebastien Dhers, Ryan M Hellyer, Jingwei Luo, Garry S Hannan, David S Larsen, and Anna L Garden

This manuscript has been accepted after peer review and appears as an Accepted Article online prior to editing, proofing, and formal publication of the final Version of Record (VoR). This work is currently citable by using the Digital Object Identifier (DOI) given below. The VoR will be published online in Early View as soon as possible and may be different to this Accepted Article as a result of editing. Readers should obtain the VoR from the journal website shown below when it is published to ensure accuracy of information. The authors are responsible for the content of this Accepted Article.

To be cited as: *Chem. Eur. J.* 10.1002/chem.201702153

Link to VoR: <http://dx.doi.org/10.1002/chem.201702153>

Supported by
ACES

WILEY-VCH

FULL PAPER

Self-Assembly of Cyclohelicate $[M_3L_3]$ Triangles over $[M_4L_4]$ Squares, despite near Linear bis-terdentate L and Octahedral M

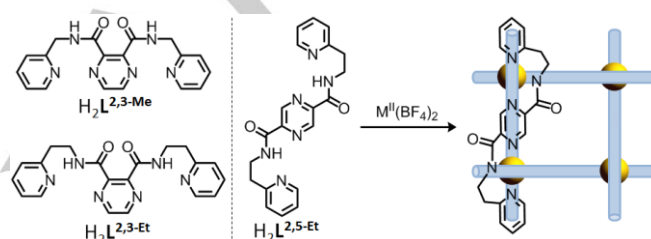
Ross W. Hogue,^[a] Sebastien Dhers,^[a] Ryan M. Hellyer,^[a] Jingwei Luo,^{[b], [c]} Garry S. Hanan,^[c] David S. Larsen,^[a] Anna L. Garden*^[a] and Sally Brooker*^[a]

Abstract: Self-assembly of 1:1:2 $M^{II}(BF_4)_2$ ($M = Zn$ or Fe), pyrazine-2,5-dicarbaldehyde (**1**) and 2-(2-aminoethyl)pyridine gave trimetallic triangle architectures rather than the anticipated tetrametallic $[2 \times 2]$ squares. Options for the non-trivial synthesis of **1** are considered, and synthetic details provided for both preferred routes. Rare *cyclohelicate* triangle architectures are observed for the pair of structurally characterized yellow-brown $[Zn_3L_3](BF_4)_6$ and dark green $[Fe_3L_3](BF_4)_6$ complexes of the neutral bis-terdentate Schiff base **L**. In order to form these pyrazine-edged triangles, the octahedral metal ions – with all 6 N-donors provided by the terdentate binding pockets of two **L** – are located 0.4–0.5 Å out of the plane of the bridging pyrazines, towards the centre of the triangle. Density functional theory calculations confirm that simple particle counting entropic arguments, which predict triangles over squares, are correct here, with the triangles shown to be energetically favored over the corresponding squares. However, importantly, DFT analysis of these and related triangle vs square systems also show that *vibrational contributions to entropy dominate* and may significantly influence the preferred architecture, such that simple particle counting *cannot in general* be reliably employed to predict the observed architecture.

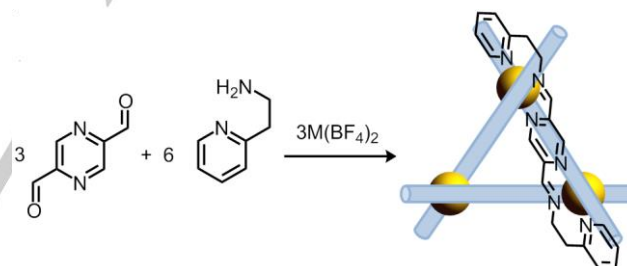
Introduction

Coordination-driven self-assembly has been used by many chemical disciplines to target specific molecular architectures.^[1] The outcomes of self-assembly are, to a large degree, governed by the directionalities of carefully designed ligands and the predictable coordination geometries of metal centers, and by entropy, which is simply expected to favor smaller polygons. Of particular interest to this research group are tetrametallic $[2 \times 2]$ grids and squares as they can provide an array of addressable magnetically interesting and/or redox-active metal centers.^[2] Previously we have reported a family of *bis-terdentate pyrazine-diamide ligands* which have generated $[2 \times 2]$ grids and squares upon self-assembly with octahedral metal ions (Scheme 1).^[3]

Here we report on the self-assembly of **L**, the *di-imine analogue* of the *diamide* $H_2L^{2,5-Et}$ (Scheme 1) with octahedral metal ions (Scheme 2). Whilst **L** is neutral and expected to be far softer than the deprotonated diamido analogues, it was expected to also form $[2 \times 2]$ square cyclohelicates with octahedral metal ions. Surprisingly, this was not the case: *instead triangular cyclohelicates* are obtained (Scheme 2), contrary to expectations based on the directional bonding approach^[1c] and the molecular library model.^[1d]



Scheme 1. Self-assembly of $M^{II}(BF_4)_2$ and pyrazine-based ditopic bis-terdentate diamide ligands $H_2L^{2,5-Et}$, $H_2L^{2,3-Me}$ and $H_2L^{2,3-Et}$ results in $[2 \times 2]$ grids (2,3-isomers) or squares (2,5-isomer).



Scheme 2. Self-assembly of a 1:1:2 mixture of metal(II) tetrafluoroborate, pyrazine-2,5-dicarbaldehyde and 2-(2-aminoethyl)pyridine results in $[M_3L_3](BF_4)_6$ triangles.

Most reported triangle metal complexes fall into one of two categories^[1h, 1i, 1k] (Figure 1): (a) those with linear metal edges and ditopic angular linking ligand corners (Figure 1, a), and (b) those with ditopic linear edge ligands and metal ion corners 'capped' with ancillary ligands (Figure 1, b). In contrast, a rare category of molecular triangle is that in which the three bridging ligands provide a complete donor set to the metal ions (Figure 1, c). Within this last class, *in which all donors are provided by just the three bridging ligands*, there are only two examples containing octahedral metal ions.^[4] The linker ligands of the triangle typically bind one metal ion from above and one metal ion from below the M_3 plane, thus forming a chiral trinuclear cyclohelicate (Figure 1, c), usually obtained as a racemic mixture. A triangular complex *with all donor atoms supplied by the three linker ligands* is the most appealing design to generate *stable* complexes for magnetic and redox applications.

[a] Ross W. Hogue, Dr Sebastien Dhers, Ryan M. Hellyer, Prof David S. Larsen, Dr Anna L. Garden and Prof Sally Brooker
Department of Chemistry and MacDiarmid Institute for Advanced Materials and Nanotechnology, University of Otago
PO Box 56, Dunedin 9054, New Zealand
E-mail: sbrooker@chemistry.otago.ac.nz

[b] Jingwei Luo
Department of Chemistry, University of Victoria, Victoria, Canada
[c] Prof Garry S. Hanan, Département de Chimie, Université de Montréal, Québec, Canada

Supporting information for this article is given via a link at the end of the document.

FULL PAPER

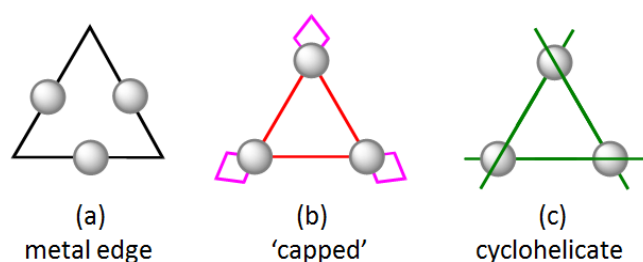


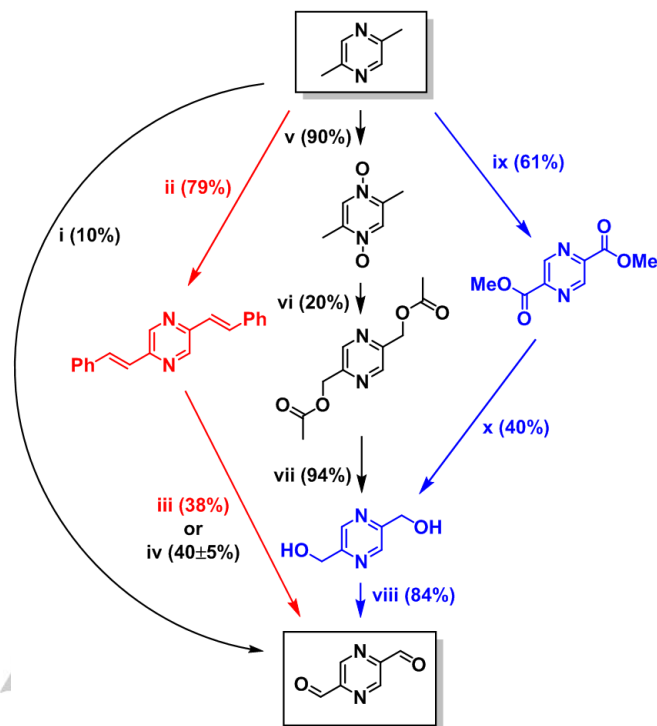
Figure 1. (a): Triangles with angular corner ligands (black). (b): Triangles with linear linker ligands (red) and metal ions which also bind 'capping' ancillary ligands (pink). (c): Trinuclear cyclohelicates with all donors from 3 ligands.

Results and Discussion

Pyrazine-2,5-dicarbaldehyde (**1**) is of significant interest as a synthetic building block. Recently it has been made via ozonolysis of 2,5-distyrylpyrazine and used as the basis of ligands designed for supramolecular chemistry.^[5] The synthesis of **1** is non-trivial (Scheme 3, see SI for discussion of the routes),^[5a, 6] but is key to the triangle complexes reported herein. Hence detailed, reliable protocols for preparing **1** via ozonolysis and also via pyrazine-2,5-diester, were established (see SI for experimental details). The ester route has the advantage of being safer to scale up, but has four steps with an overall yield of 20% (Scheme 3, blue). The ozonolysis route has its associated hazards, but only requires two steps and proceeds in a better overall yield of 31% (Scheme 3, red).

Both $[\text{Zn}_3\text{L}_3](\text{BF}_4)_6$ and $[\text{Fe}_3\text{L}_3](\text{BF}_4)_6$ are made by one pot reactions of a 1:2:1 ratio of **1**, 2-(2-aminoethyl)pyridine and $\text{M}^{\text{II}}(\text{BF}_4)_2 \cdot x\text{H}_2\text{O}$ ($\text{M} = \text{Zn}$ or Fe), in MeCN. Subsequent vapor diffusion of Et_2O into these solutions over a few days gives pale-tan block-like single crystals for Zn(II), and green plate-like single crystals for Fe(II). Single crystal X-ray diffraction studies on both complexes unexpectedly revealed the structures to be *rare examples of triangular cyclohelicates* (Figure 2), rather than the anticipated $[2 \times 2]$ squares. Cryospray mass spectrometry was consistent with M_3L_3 triangles, with peaks corresponding to $\{[\text{M}_3\text{L}_3](\text{BF}_4)_5\}^+$ and $\{[\text{M}_3\text{L}_3](\text{BF}_4)_4\}^{2+}$ observed for both compounds (Figures S4-S6 and S10-S11): in no case were M_4L_4 or higher order species detected (Figures S7-S9 and S12-S13). Both compounds have been further characterized by elemental analysis, IR, UV-vis, and ^1H and ^{13}C NMR spectroscopies (ESI).

The asymmetric unit of $[\text{Zn}_3\text{L}_3](\text{BF}_4)_6$ contains one $\text{Zn}^{\text{II}}\text{L}$ component, which represents one third of the triangle, with the other two thirds generated by a 3-fold rotation axis through the center of the triangle, at right angles to the Zn_3 plane. All donors to each octahedral Zn(II) are provided by two N_3 pockets from two different **L** ligands. The cyclohelical architecture imparts inherent chirality to the $[\text{Zn}_3\text{L}_3](\text{BF}_4)_6$ triangle. All Zn(II) ions are chiral-at-metal with all ions within one complex cation having the same chirality. The complex crystallized in the R-3 space group, so is racemic, with inversion generating a 50:50 mixture of $(\Delta\Delta\Delta)$ and $(\Lambda\Lambda\Lambda)$ enantiomers.



Scheme 3. The available synthetic routes to pyrazine-2,5-dicarbaldehyde. Conditions (yield): (i) V_2O_5 , MoO_3 , AgO_2 catalyst, O_2 (10%).^[6a, 6b] (ii) benzaldehyde, benzoic anhydride, reflux (79%).^[6c, 6d] (iii) a: O_3 , MeOH, -78°C , b: $\text{Na}_2\text{S}_2\text{O}_5$, continuous extraction (38%).^[5a, 6e] (iv) OsO_4 , NaIO_4 , THF/ H_2O (2:1), Ar (40±5%).^[6f] (v) m-CPBA, EtOAc (90%).^[6g] (vi) Ac_2O , 158°C (20%).^[6h] (vii) NaOMe, dry MeOH (94%).^[6g] (viii) MnO_2 , CHCl_3 , reflux (84%).^[6g] (ix) SeO_2 , pyridine/water (10:1), reflux (61%). (x) a: NaBH_4 , MeOH, b: H_2O , continuous extraction (40%).^[6h]

X-ray crystal structure analysis showed that coordination of **L** to Fe(II) results in a trimetallic triangular complex, $[\text{Fe}_3\text{L}_3](\text{BF}_4)_6$. Here the asymmetric unit contains one and a half $\text{Fe}^{\text{II}}\text{L}$ units, with the other half of the triangle formed by 2-fold rotation (Figure 2). All of the Fe-N bonds are ca. 2.0 Å and $\Sigma = 45.4^\circ$ (Table 1), characteristic of low spin (LS) Fe(II). As with the Zn(II) complex, $[\text{Fe}_3\text{L}_3](\text{BF}_4)_6$ is a chiral cyclohelicate in which the three Fe(II) ions within one complex cation have the same configuration, and a 50:50 mixture of $(\Delta\Delta\Delta)$ and $(\Lambda\Lambda\Lambda)$ enantiomers are observed in the crystal lattice due to inversion symmetry (C_2/m).

Ligands providing a bridging pyrazine moiety provide these two N donor atoms at 180° (Scheme 2), so, according to the directional bonding approach^[1c] and the molecular library model,^[1d] assembly with octahedral metal ions is expected to produce molecular *squares*. The formation of molecular *triangles* instead must be the result of either (a) the pyrazine directional angle deviating from 180° (edges) and/or (b) the $\text{N}_{\text{pz}}\text{-M-N}_{\text{pz}}$ corner angles deviating from 90° (square) towards 60° (triangle). Indeed the $\text{N}_{\text{pz}}\text{-M-N}_{\text{pz}}$ corners are less than 90° for both compounds $\{[\text{Zn}_3\text{L}_3], 79.6^\circ(1); [\text{Fe}_3\text{L}_3], \text{av. } 85.1^\circ(1)\}$, but these modest deviations clearly cannot account for how these triangles have been obtained. Rather, it is the deviation of the binding of pyrazine edges away from 180° directionality that is the key here.

FULL PAPER

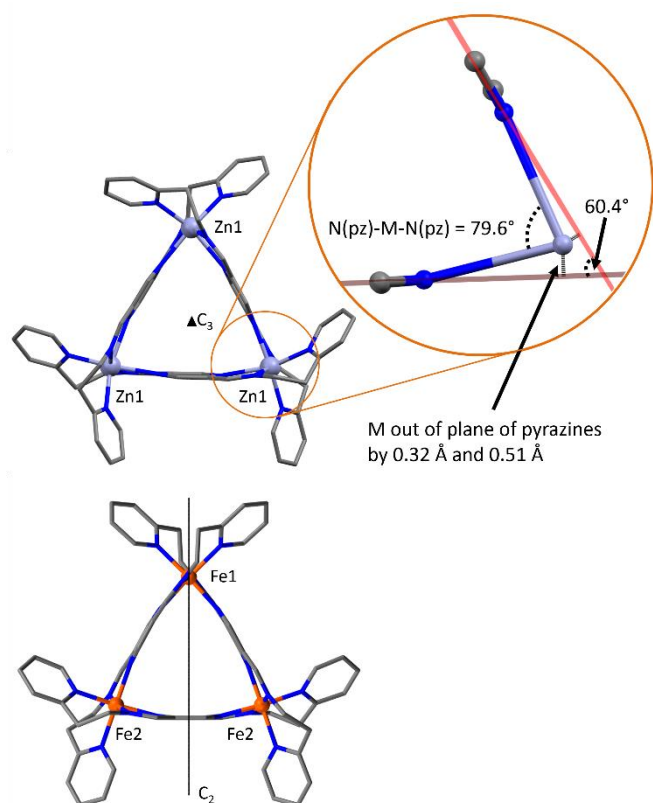


Figure 2. Perspective view of the hexacations of $[\text{Zn}_3\text{L}_3](\text{BF}_4)_6$ (top, including an expansion of one corner, displaying $N_{\text{pz}}\text{-M-N}_{\text{pz}}$ and pyrazine-pyrazine mean plane angles, and the M out of plane pyrazine distances) and $[\text{Fe}_3\text{L}_3](\text{BF}_4)_6$ (bottom). Zn (light indigo), Fe (red), N (blue) and C (grey). Hydrogen atoms omitted for clarity. Symmetry operations (top) 3-fold rotation axis running through the center of the triangle perpendicular to the M_3 plane, and (bottom) 2-fold rotation axis running through Fe1 only in the M_3 plane.

In all cases the metal center sits significantly out of the plane of the attached pyrazine rings towards the center of the triangle (Figure 2), on average by 0.41 Å for $[\text{Zn}_3\text{L}_3]$ and 0.46 Å for $[\text{Fe}_3\text{L}_3]$. In contrast the square $[\text{Co}^{\text{II}}_4(\text{L}^{2,5\text{-Et}})_4](\text{BF}_4)_4$ obtained when the analogous pyrazine di-amide ligand was employed (Scheme 1),^[3b] has $N_{\text{pz}}\text{-M-N}_{\text{pz}}$ angles (av. 87.52°) closer to 90° and metal ions only 0.07 Å out the plane of the two coordinated pyrazine rings (Table 1). In summary, these results show that the 2,5-pyrazine bridging moiety in these imine and amide bis-terdentate ligands is not geometrically predisposed towards only one architecture, as either triangles or squares can be achieved.

A survey of the literature [CSD search for triangles comprising three metal ions bridged by any bonds to three pyrazine rings (Figure S26); CSD version 5.38 updates (November 2016)] revealed only four other structurally characterized pyrazine-edge triangle complexes: two with square planar metal ions, $[\text{Rh}_3(\text{PPh}_3)_6(\mu\text{-pz})_3](\text{ClO}_4)_3$ ^[7] and $[\{\text{Pt}(\text{PMe}_3)_2(\mu\text{-pz})\}_3](\text{CF}_3\text{SO}_3)_6$ ^[8] and two with octahedral metal ions, $[\{\text{trans},\text{cis-RuCl}_2(\text{dmsO-S})_2(\mu\text{-pz})\}_3]$ ^[9] and $[\{\text{ZnCl}_2(\text{PPh}_3)_2(\mu\text{-bppz})\}_3]$ ^[10] (Table S3).

Table 1. Comparison of selected distances (Å) and angles (°) for compounds $[\text{Zn}_3\text{L}_3](\text{BF}_4)_6$, $[\text{Fe}_3\text{L}_3](\text{BF}_4)_6$, and $[\text{Co}^{\text{II}}_4(\text{L}^{2,5\text{-Et}})_4](\text{BF}_4)_4$ (See Table S2 for more details).

	$[\text{Zn}_3\text{L}_3](\text{BF}_4)_6$	$[\text{Fe}_3\text{L}_3](\text{BF}_4)_6$ ^[a]	$[\text{Co}^{\text{II}}_4(\text{L}^{2,5\text{-Et}})_4](\text{BF}_4)_4$
Reference	This work	This work	[3b]
cis-N-M-N range; [av.]	73.70(10)-105.26(10); [89.70]	81.24(9)-95.32(9); [89.99]/80.82(9)-96.24(9); [90.03]	81.94(14)-94.38(15); [89.98]
$N_{\text{pz}}\text{-M-N}_{\text{pz}}$	79.6(1)	84.33(13)/85.87(9)	87.52(14)
Av. M out of plane pz ^[b]	-0.41	-0.46	0.07

[a] Fe1/Fe2. [b] Negative value indicates M is on the inside face of the plane, closer to center of triangle/square.

In each case a molecular square was anticipated by the authors, however, much like the present cyclohelicates, $N_{\text{pz}}\text{-M-N}_{\text{pz}}$ angles closer to 80° (80.47°-85.98°, av. 82.05°) in combination with the metal ions being located out of the pyrazine planes (0.23-0.66 Å, av. 0.44 Å), facilitated the formation of triangles instead. All four of these literature examples are 'capped' triangles, and the bulky 'caps' had been postulated to predispose the metal corners towards angles more suited to triangles over squares.^[11]

In contrast, here we report the first examples of structurally characterized pyrazine-edged triangular cyclohelicates (Figure 1 c), in which all six donor atoms to each metal ion are provided by the di-imine bis-terdentate pyrazine-edge ligands L. This triangle architecture contrasts with the molecular squares that the closely analogous diamide bis-terdentate ligands, $\text{H}_2\text{L}^{2,5\text{-Et}}$ ^[3b] and $\text{H}_2\text{L}^{2,3\text{-Me}}$ or Et^[3a, 3c, 11] (Scheme 1), generated upon complexation with octahedral metal ions. The only pyrazine-edged triangular cyclohelicate, $[\text{Zn}_3(\text{bbppz})_3](\text{PF}_6)_6$ (bbppz is 2,5-bis([2,2']bipyridin-6-yl)pyrazine), reported previously was only observed in solution as the minor product in equilibrium with the (structurally characterized) Zn^{II}_4 square.^[4a]

To gain further insight into the subtle factors contributing to whether a triangle or square architecture is realized, density functional theory (DFT) calculations on the $[\text{Zn}_3\text{L}_3]^{6+}$ and $[\text{Fe}_3\text{L}_3]^{6+}$ triangles, and the corresponding (but not observed) $[\text{Zn}_4\text{L}_4]^{8+}$ and $[\text{Fe}_4\text{L}_4]^{8+}$ squares were performed with a continuum acetonitrile solvent model. The GGA functional BP86,^[12] which is known to perform well with transition metal complexes,^[13] was used with a def2-SVP basis set.^[14]

The total electronic energies, E , are reported as 'per ML unit', i.e. the total energies of the triangles and squares are divided by three and four respectively to account for the stoichiometry. Optimized structures of $[\text{Zn}_3\text{L}_3]^{6+}$ and $[\text{Fe}_3\text{L}_3]^{6+}$ have very similar geometries to the crystallographic data (Tables S5-S6). Despite showing a significant deviation from the ideal 180° directional bonding in the bridging pyrazine unit, the optimized triangles both have lower E (per ML unit) than the corresponding $[\text{Zn}_4\text{L}_4]^{8+}$ and $[\text{Fe}_4\text{L}_4]^{8+}$ squares by 3.42 and 4.05 kJ mol⁻¹ respectively (Tables 2 and S4). The results of the DFT calculations are therefore consistent with the experimentally observed triangle architectures.

FULL PAPER

The same DFT analysis was applied to the related pyrazine-edged squares, $[\text{Co}_4(\text{L}^{2,5\text{-Et}})_4]^{4+}$,^[3b] $[\text{Zn}_4(\text{bbppz})_4]^{8+}$,^[4a] and $[\text{Fe}^{\text{II}}_4(\text{bbppz})_4]^{8+}$,^[15] as well as the corresponding (but not structurally characterized and/or observed) triangles, and the total electronic energies were also consistent with the reported architecture outcomes (Table S4).

Table 2. Total electronic energy, ΔH , and ΔS relative to the square complex for each M+L combination. Rotational, translational, and vibrational contributions to overall entropy are detailed. All are per ML (kJ mol^{-1})

	$[\text{Zn}_3\text{L}_3]^{6+}$	$[\text{Zn}_4\text{L}_4]^{8+}$	$[\text{Fe}_3\text{L}_3]^{6+}$	$[\text{Fe}_4\text{L}_4]^{8+}$
E^{rel}	-3.42	0 (by def.)	-4.05	0 (by def.)
H^{rel}	-4.37	0 (by def.)	-7.53	0 (by def.)
TS^{el}	≈ 8	0 (by def.)	≈ 8	0 (by def.)
TS_{rot}	16.50	12.74	16.34	12.61
TS_{trans}	19.63	14.99	19.60	14.96
TS_{vib}	≈ 100	≈ 100	≈ 100	≈ 100

To probe the competing energetic influences, the relative enthalpic and entropic stabilities were evaluated using the DFT-calculated data and ideal gas statistical mechanics (Table 2 and Table S4). In all five cases, the enthalpic product was the same as that predicted by consideration of electronic energy E alone. Despite the subcomponents deviating from their ideal bonding geometries, the triangles $[\text{Zn}_3\text{L}_3]^{6+}$ and $[\text{Fe}_3\text{L}_3]^{6+}$ are calculated to have lower enthalpy than the corresponding squares. Explanations for this are difficult as enthalpic contributions are often complex and can involve geometric strain,^[16] internal void space,^[4a] and hydrophobic effects upon changing surface area to volume ratios.^[17] For these reasons we refrain from using ΔH to calculate Gibb's energies.

For all five cyclohelicates the triangle was found to be the *entropically-favored* product (Table 2 and Table S4). This is no surprise, as it is generally accepted that dynamic mixtures of molecular polygons entropically favor smaller assemblies due to the greater number of discrete molecules formed (4 triangles vs 3 squares from a mixture of 12M + 12L).^[1d, 1h, 1j, 1l] However, we note that the calculation of entropy for these complexes is difficult as they have very many low-frequency modes which are not well-described within standard thermochemical models such as those used here. Despite these inherent uncertainties, *it is clear that the vibrational contributions, $TS_{\text{vib}} \approx 100 \text{ kJ mol}^{-1}$* (Table 2), are much larger than the rotational and translational contributions, TS_{rot} and TS_{trans} , *so are the dominant contributor to the overall entropy of these cyclohelicates.* So, whilst DFT indicates that in all cases the triangles are entropically favored over the squares, in fact this may or may not be the case.

This observation may provide some insight into some previously puzzling results, where *larger cyclohelicate assemblies were reported to be entropically favored*,^[4a, 18] a result described by those authors as counterintuitive, but one which might be explained by low frequency vibrational modes tipping the overall entropy in favor of the larger molecular assemblies, i.e. the *dominance of the vibrational contribution to the overall entropy, as shown herein*, indicates that the different vibrational properties of the different sized cyclohelicates may influence the entropic

preference to such an extent that *particle counting arguments are not sufficient to explain the observed product.*

Conclusions

Rather than the *square [2x2] cyclohelicates* that were anticipated, and indeed *seen for the analogous di-amide ligand*, the *first examples of pyrazine-based triangle cyclohelicates* were unexpectedly obtained on self-assembly of a new bis-terdentate pyrazine *di-imine* ligand with octahedral metal ions. Careful analysis of the structures of these triangles reveals that the pyrazine bridging moiety of this bis-terdentate ligand is quite flexible, accommodating the binding of octahedral metal ions either *in* (square, related ligands), or *well out* (triangles, this study) *of the plane of the pyrazine ring.*

DFT analysis of both the observed triangles and the corresponding squares, as well as of related reported pyrazine cyclohelical triangles/squares, *correctly predicts the observed architectures.* However, these DFT calculations also show that *vibrational contributions, which are difficult to model, dominate the overall entropy, so, in general, simple counting arguments (which favor more smaller assemblies) cannot be reliably employed in the prediction of architecture outcomes.*

Subtle variations of these bis-terdentate donor sets are currently underway as fine-tuning of both the field strength and geometric control will enable further probing of this assembly algorithm and the formation of magnetically interesting, rather than diamagnetic, metal complexes.

Experimental Section

General experimental details

The solvents used were reagent grade and were used as received from commercial suppliers. NaBH_4 (97%) and SeO_2 (97%) were purchased from Ajax Finechem. MnO_2 (85%, particle size < 5 μm) was purchased from Sigma-Aldrich. All other chemicals were reagent grade and were used as received from commercial suppliers. All reactions were conducted in air unless otherwise stated.

IR spectra were recorded as solids on a Bruker Alpha FT-ATR IR spectrometer with a diamond anvil Alpha-P module between 400 and 4000 cm^{-1} . The ^1H and ^{13}C NMR spectra at 25 $^\circ\text{C}$ were recorded on a Varian 400 MHz spectrometer. Standard microanalysis was carried out by the Campbell Microanalytical Laboratory at the University of Otago. Mass spectrometry was recorded by Professor Garry Hanan at the University of Montreal, Canada using a MicrOTOF II mass spectrometer from Bruker in positive ion mode using pneumatically assisted CryoSpray source: Capillary voltage, 4500 V; End Plate Offset -500V; Capillary Exit voltage, 20 V; dry gas temperature, -20 to 0 $^\circ\text{C}$; Nebulizer gas temperature, -60 to -20 $^\circ\text{C}$; Nebulizer gas flow, 0.150 MPa; dry gas flow, 1.5 L/min.

X-ray crystallographic data were collected on Bruker Kappa Apex II CCD area detector diffractometer (University of Otago). In both cases graphite-monochromated Mo KR radiation ($\lambda = 0.71073 \text{ \AA}$) was used. The data were collected at 85 K. All data sets were corrected for absorption using SADABS.^[19] Structures were solved using SUPERFLIP and refined against all F^2 data (except for the Zn structure in which OMIT 0 1 2 was used due to this reflection being partially obscured by the beamstop) using

FULL PAPER

SHELX-2014.^[20] All non-H atoms were refined with anisotropic thermal parameters. All H atoms were inserted at calculated positions and rode on the C atoms to which they were attached with thermal parameters equal to 1.2 times that of the parent atom. Owing to the presence of badly disordered lattice solvent molecules and significant unassignable Q peaks, the structures were treated with SQUEEZE^[21] (see SI for details). High-resolution pictures were prepared using Mercury^[22] and POVray^[23] software. CCDC 1530644-1530645.

Synthesis details

2,5-Distyrylpyrazine.^[6d] A mixture of 2,5-dimethylpyrazine (6.27 g, 58.0 mmol), benzaldehyde (20.37 g, 192.0 mmol) and benzoic anhydride (22.19 g, 97.9 mmol) was refluxed overnight. After cooling to room temperature, it was filtered and the black/yellow filter cake washed with methanol (3 x 50 mL) then diethyl ether (1 x 25 mL) to give the product as a yellow powder (8.95 g, 54%, which should be stored in the dark). Found: C 84.50, H 5.78, N 10.04%. Calculated for C₂₀H₁₆N₂ (284.36 g mol⁻¹): C 84.48, H 5.67, N 9.85%. ¹H NMR (400 MHz, CDCl₃): δ(ppm) = 8.60 (s, 2H, H_A), 7.74 (d, *J* = 7.7 Hz, 1H, H_B), 7.61 (d, *J* = 7.3 Hz, 2H, H_C), 7.40 (t, *J* = 7.3 Hz, 2H, H_E), 7.34 (d, *J* = 7.3 Hz, 1H, H_F), 7.19 (d, *J* = 7.7 Hz, 1H, H_C).

Pyrazine-2,5-dicarbaldehyde.^[6e] *Caution: ozonolysis is a reaction that proceeds through the formation of an explosive intermediate, an organic ozonide, making it an extremely dangerous reaction to scale up. Consequently, the reaction should be done on a small scale (never use more than 2 g of starting material), a blast shield should be used during the reaction and extreme precaution should be taken.* Behind a blast shield, a pale yellow suspension of 2,5-distyrylpyrazine (1.90 g, 6.68 mmol) in methanol (300 mL) was chilled in a dry ice/acetone bath and then treated with ozone for 10 minutes, turning the suspension blue. Nitrogen was then bubbled through for a period of 30 minutes to remove the excess ozone, giving back the original yellow colour. Next, 2 mL of a freshly prepared aqueous solution of sodium metabisulfite (23% by mass) was added dropwise and the reaction mixture allowed to warm up to room temperature whilst still under nitrogen. The mixture was filtered and the filtrate was taken to dryness under reduced pressure. Saturated NaCl solution (10 mL) was added and used to rinse the resulting yellow solid into a separating funnel. The aqueous layer was washed with diethyl ether (3 x 50 mL) to remove the benzaldehyde byproduct, and then continuously extracted with chloroform for 1 day. The chloroform fraction was taken to dryness to give the product as a yellow solid (350 mg, 2.52 mmol, 38%). Found: C 53.20, H 3.26, N 20.33%. Calculated for C₆H₄N₂O₂ (139.11 g mol⁻¹): C 52.95, H 2.96, N 20.58%. ¹H NMR (400 MHz, CDCl₃): δ(ppm) = 10.22 (s, 2H, CHO), 9.29 (s, 2H, PzH).

Dimethylpyrazine-2,5-dicarboxylate. *Caution: SeO₂ is toxic and should be handled with care. If spilled, use dry sand and collect the spilled material to put it in a sealed container, and then dispose of it in a secured sanitary landfill.* To a light yellow solution of 2,5-dimethylpyrazine (8.11 g, 75.0 mmol) in pyridine (150 mL) was added solid selenium dioxide (37.5 g, 338 mmol) and water (15 mL) and the resulting suspension refluxed for 18 hours. The resulting dark red-brown mixture was evaporated to dryness under reduced pressure. Water (250 mL) was added and the solid elemental selenium was filtered off. The red filtrate was evaporated to dryness. The resulting dark red-brown solid was taken up in methanol (150 mL), thionyl chloride (4.6 mL) added and the suspension refluxed for 8 hours. The resulting suspension was hot filtered and the solid residue washed with dichloromethane (5 x 20 mL). The combined organic phases were reduced to 100 mL under reduced pressure to give pale yellow orange feathery crystals. The solid was filtered off and washed with ice-cold methanol (30 mL) to give 8.98 g (45.8 mmol, 61%) of analytically pure

dimethylpyrazine-2,5-dicarboxylate. Found: C 49.24, H 3.87, N 14.25%. Calculated for C₈H₈N₂O₄ (196.16 g mol⁻¹): C 48.98, H 4.11, N 14.28%. ¹H NMR (300 MHz, CD₃Cl₃): δ(ppm) = 9.39 (s, 2H, PzH), 4.07 (s, 6H, CH₃). ¹³C NMR (100 MHz, CD₃Cl₃): δ(ppm) = 163.6 (PzCO), 145.6 (PzH), 145.3 (PzCO), 53.6 (OCH₃).

2,5-Bis(hydroxymethyl)pyrazine.^[6h] Dimethylpyrazine-2,5-dicarboxylate (1.0 g, 5.1 mmol) was dissolved in methanol (40 mL). The solution was chilled in an ice bath then NaBH₄ (1.54 g, 40.8 mmol) was added slowly with stirring over 15 minutes. The ice bath was removed after around an hour, when all the ice was melted. After stirring overnight, 5 mL of water was added and the solution left to stir for 10 minutes then taken to dryness under reduced pressure. The residue was then dissolved in 2.5 mL of water and continuously extracted with chloroform for 2 days. 2,5-Bis(hydroxymethyl)pyrazine was collected as a pale yellow solid (280 mg, 40%). Found: C 50.26, H 5.53, N 19.11%. Calculated for C₆H₈N₂O₂·H₂O (143.36 g mol⁻¹): C 50.13, H 5.89, N 19.41%. ¹H NMR (500 MHz, CD₃OD): δ(ppm) = 8.65 (s, 2H, PzH), 4.76 (s, 4H, CH₂), 4.85 (s, 2H, OH). ¹³C NMR (500 MHz, CD₃OD): δ(ppm) = 156.1 (PzCH₂), 142.8 (PzH), 64.0 (CH₂).

Pyrazine-2,5-dicarbaldehyde (1). To a yellow solution of 2,5-bis(hydroxymethyl)pyrazine (280 mg, 2.0 mmol) in dry chloroform (50 mL) was added manganese dioxide (1.7 g, 19.5 mmol). The resulting suspension was stirred and refluxed for 3 hours. The resulting mixture was filtered (celite on sinter) and the solid washed with chloroform (2 x 50 mL). The combined filtrate was taken to dryness *in vacuo* yielding 275 mg of the product as a yellow solid (1.69 mmol, 84%). Found: C 52.21, H 3.41, N 19.76%. Calculated for C₆H₄N₂O₂·1.5H₂O (163.13 g mol⁻¹): C 51.92, H 3.12, N 20.18%. ¹H NMR (500 MHz, CDCl₃): δ(ppm) = 10.232, s (CHO), 9.302, s (PzH). ¹³C NMR (125 MHz, CDCl₃): δ(ppm) = 191.63 CHO, 148.60 Pz, 143.24 PzH.

[Zn₃L₃](BF₄)₆. To a stirred solution of pyrazine-2,5-dicarbaldehyde (10.0 mg, 73.5 μmol) in CH₃CN (10 mL) was added 2-(2-aminoethyl)pyridine (17.2 μL, 147 μmol) in CH₃CN (155 μL). After 20 min, a solution of Zn(BF₄)₂·H₂O (17.6 mg, 73.5 μmol) in CH₃CN (1 mL) was added, giving a pale tan-brown coloured solution which darkened on stirring for 30 min. Vapour diffusion of Et₂O into this solution over 4 days gave brown crystals in a yellow coloured solution. The solvent was decanted off and the solids dried *in vacuo* affording [Zn₃L₃](BF₄)₆ as a tan-brown coloured solid (yield 36 mg, 84.0%). ¹H NMR (CD₃NO₂, 500 MHz): δ = 3.16 (m, 2H, CH₂), 3.36 (d, 2H, CH₂, ³J = 16 Hz), 4.49 (m, 2H, CH₂), 4.65 (d, 2H, CH₂, ³J = 18 Hz), 7.35 (m, 2H, PyH), 7.56 (d, 2H, PyH, ³J = 8 Hz), 7.99 (m, 2H, PyH), 8.08 (d, 2H, PyH, ³J = 5.5 Hz), 8.34 (s, 2H, PzH) and 8.80 ppm (d, 2H, ImH, ³J = 2 Hz). ¹³C NMR (CD₃NO₂, 133 MHz): δ = 34.77 (CCH₂), 57.521 (CCH₂), 125.373 (C_{Py}), 127.911 (C_{Py}), 142.31 (C_{Py}), 145.75 (C_{Pz}), 146.937 (C_{Pz}), 149.44 (C_{Py}), 161.324 (C_{Py}), 164.165 ppm (C_{Im}). Elemental analysis. Found: C, 41.87; H, 3.70; N, 14.67%. Calculated for C₆₀H₆₀N₁₈Zn₃B₆F₂₄·CH₃CN: C, 41.57; H, 3.54; N, 14.86%. IR ν_{CN} (ATR, cm⁻¹): 1645 (m) 1609 (m) 1572 (w) 1488 (m) 1445 (m) 1404 (m) 1309 (m) 1188 (m) 1019 (s) 879 (m) 841 (m) 784 (w) 767 (m). UV/Vis (CH₃CN): λ_{max} (ϵ) = 240 (45389), 324 (41259 L mol⁻¹cm⁻¹). Cryospray-MS (+): *m/z* = 1662.3074 {[Zn₃L₃](BF₄)₅}⁺ (calcd = 1662.3276), 788.1550 {[Zn₃L₃](BF₄)₄}²⁺ (calcd = 778.1610), 496.4363 {[Zn₃L₃](BF₄)₃}³⁺ (calcd = 496.4393), 350.5771 {[Zn₃L₃](BF₄)₂}⁴⁺ (calcd = 350.5785).

[Fe₃L₃](BF₄)₆. To a stirred solution of pyrazine-2,5-dicarbaldehyde (10.0 mg, 73.5 μmol) in CH₃CN (10 mL) was added 2-(2-aminoethyl)pyridine (17.2 μL, 147 μmol) in CH₃CN (155 μL). After 30 min, a solution of Fe(BF₄)₂·6H₂O (49.6 mg, 147 μmol) in CH₃CN (1 mL) was added, giving an intense dark green coloured solution which was left to stir overnight before concentration down to half the volume *in vacuo*. Vapour diffusion of Et₂O into this solution over 3 days gave green single plate-like crystals in a colourless solution. The solvent was decanted off and the solids dried *in vacuo* giving [Fe₃L₃](BF₄)₆ as a dark green coloured solid (yield 22 mg,

FULL PAPER

52 %). ^1H NMR (CD_3CN , 400 MHz): δ = 2.76 (m, 2H, CH_2), 3.38 (d, 2H, CH_2 , 3J = 16.0 Hz), 4.32 (m, 2H, CH_2), 5.18 (d, 2H, CH_2 , 3J = 16.0 Hz), 7.11 (m, 2H, PyH), 7.42 (d, 2H, PyH, 3J = 7.3 Hz), 7.56 (d, 2H, PzH, 3J = 5.0 Hz), 7.83 (m, 4H, PyH) and 9.76 ppm (s, 2H, ImH). ^{13}C NMR (CD_3CN , 133 MHz): δ = 34.51 (C_{CH_2}), 57.18 (C_{CH_2}), 123.53 (C_{Py}), 127.79 (C_{Py}), 140.16 (C_{Py}), 151.03 (C_{Py}), 153.37 (C_{Py}), 155.58 (C_{Pz}), 165.12 (C_{Pz}), 172.67 ppm (C_{Im}). Elemental analysis calcd for $\text{C}_{60}\text{H}_{60}\text{N}_{18}\text{Fe}_3\text{B}_6\text{F}_{24}$: C 41.86, 3.51, 14.64%; found: C 41.68, H 3.74, N, 14.84%. IR u_{CN} (ATR, cm^{-1}): 1608 (m) 1569 (w) 1484 (m) 1443 (m) 1363 (w) 1317 (w) 1303 (w) 1206 (m) 1030 (s) 927 (m) 761 (m). UV/Vis (CH_3CN): λ_{max} (ϵ) = 254 (16775), 300 (12750), 433 (6250), 623 (5250), 721 nm (4750 $\text{L mol}^{-1}\text{cm}^{-1}$). Cryospray-MS (+): m/z = 1635.3403 $\{[\text{Fe}_3\text{L}_3](\text{BF}_4)_3\}^+$ (calcd = 1635.3479), 774.1794 $\{[\text{Fe}_3\text{L}_3](\text{BF}_4)_4\}^{2+}$ (calcd = 774.1719).

DFT calculations

All DFT calculations were performed using the ORCA program version 3.0.3.^[24] Complexes were fully optimized using the BP86^[12] functional with a def2-SVP basis set.^[14] The resolution of identity approximation^[25] was also used with a def2-SVP/J auxiliary basis set.^[26] Calculations were performed in a polarizable continuum solvent using both the COSMO^[27] and^[28] SMD solvation models, and acetonitrile as the solvent. The starting coordinates for $[\text{Zn}_3\text{L}_3]^{6+}$, $[\text{Fe}_3\text{L}_3]^{6+}$, $[\text{Co}^{\text{II}}_4(\text{L}^{2,5-\text{Et}})_4]^{4+}$, $[\text{Fe}^{\text{II}}_4(\text{bbppz})_4]^{8+}$, and $[\text{Zn}^{\text{II}}_4(\text{bbppz})_4]^{8+}$ were those from the cif file of the x-ray crystallographic data. The starting coordinates of $[\text{Zn}_4\text{L}_4]^{8+}$ and $[\text{Fe}_4\text{L}_4]^{8+}$ were those from the cif file of $[\text{Co}^{\text{II}}_4(\text{L}^{2,5-\text{Et}})_4]^{4+}$, and the starting coordinates of $[\text{Co}^{\text{III}}_3(\text{L}^{2,5-\text{Et}})_3]^{3+}$, $[\text{Fe}^{\text{III}}_3(\text{bbppz})_3]^{6+}$ and $[\text{Zn}^{\text{III}}_3(\text{bbppz})_3]^{6+}$ were those of $[\text{Zn}_3\text{L}_3]^{6+}$. Frequency calculations were carried out on all complexes to confirm they were local minima by the existence of no significant imaginary frequencies. Imaginary frequencies below 35 cm^{-1} were assumed to be due to numerical noise. No corrections were made for zero point energies or dispersion. The calculations produce total electronic energies, which are adjusted for the complex stoichiometry and reported as total energy per ML unit. All complexes were re-optimized using the B3LYP functional and the results were qualitatively the same, confirming that the relative stabilities were not artefacts of the chosen density functional.

The enthalpy, H, and entropy, S, of the cyclohelicates were derived using DFT-calculated energies and ideal gas statistical mechanics within the harmonic approximation. Vibrational modes with frequencies below 35 cm^{-1} were excluded, the number of which was between 5-18, depending on the complex. It should be noted that there remain very many low-frequency modes. Low-frequency vibrational modes are not well-described with a harmonic description therefore there exists a large degree of uncertainty in the calculated vibrational entropy. The calculated rotational, vibrational and translation entropies of the cyclohelicates are presented in Table S4. Clearly, TS_{vib} is approximately an order of magnitude larger than TS_{rot} and TS_{trans} , therefore it has the largest effect on the overall entropy of the cyclohelicates. Given that this value is highly uncertain, the overall entropy and any quantity derived from it (e.g. Gibb's energy, G) is also uncertain therefore we do not present calculated values of G here. Considering the relative enthalpy and entropy of the cyclohelicates (Table S4), it is clear that the enthalpic product is the same as predicted by the relative electronic energies, for all $\text{M}_3\text{L}_3/\text{M}_4\text{L}_4$ pairs. In all cases, the triangle is the entropically favoured cyclohelicate.

Acknowledgements

We thank the University of Otago (PhD scholarship to RWH; and Versalab magnetometer purchase), the MacDiarmid Institute for Advanced Materials and Nanotechnology (PhD scholarship to SD), and the Marsden Fund (RSNZ; PhD scholarship to RMH) for

supporting this research. We also thank the Natural Sciences and Engineering Research Council (NSERC) for financial support of the visit of JL (Victoria) to GSH (Montreal), during which the MS data were obtained, and Prof Scott McIndoe (Victoria) and Dr Joseph Lane (Waikato) for helpful advice. The authors wish to acknowledge NeSI high-performance computing facilities. NZ's national facilities are provided by the NZ eScience Infrastructure and funded jointly by NeSI's collaborator institutions and through the Ministry of Business, Innovation & Employment's Research Infrastructure programme. URL <https://www.nesi.org.nz>.

Conflict of Interest

The authors declare no competing financial interests.

Keywords: supramolecular chemistry; self-assembly; triangles; cyclohelicates; entropy

- [1] a) D. L. Caulder, K. N. Raymond, *J. Chem. Soc., Dalton Trans.* **1999**, 1185-1200; b) D. L. Caulder, K. N. Raymond, *Acc. Chem. Res.* **1999**, *32*, 975-982; c) B. J. Holliday, C. A. Mirkin, *Angew. Chem. Int. Ed.* **2001**, *40*, 2022-2043; d) S. Leininger, B. Olenyuk, P. J. Stang, *Chem. Rev.* **2000**, *100*, 853-908; e) J.-M. Lehn, *Science (Washington D.C.)* **2002**, *295*, 2400-2403; f) M. Fujita, M. Tominaga, A. Hori, B. Therrien, *Acc. Chem. Res.* **2005**, *38*, 369-378; g) J. R. Nitschke, *Acc. Chem. Res.* **2007**, *40*, 103-112; h) E. Zangrando, M. Casanova, E. Alessio, *Chem. Rev.* **2008**, *108*, 4979-5013; i) B. Lippert, P. J. Sanz Miguel, *Chem. Soc. Rev.* **2011**, *40*, 4475-4487; j) R. J. Chakrabarty, P. S. Mukherjee, P. J. Stang, *Chem. Rev.* **2011**, *111*, 6810-6918; k) N. J. Young, B. P. Hay, *Chem. Commun.* **2013**, *49*, 1354-1379; l) W. Wang, Y.-X. Wang, H.-B. Yang, *Chem. Soc. Rev.* **2016**, *45*, 2656-2693.
- [2] a) M. Ruben, J. Rojo, F. J. Romero-Salguero, L. H. Uppadine, J.-M. Lehn, *Angew. Chem. Int. Ed.* **2004**, *43*, 3644-3662; b) M. Ruben, J.-M. Lehn, P. Müller, *Chem. Soc. Rev.* **2006**, *35*, 1056-1067; c) L. N. Dawe, T. S. M. Abedin, L. K. Thompson, *Dalton Trans.* **2008**, 1661-1675; d) L. N. Dawe, K. V. Shuvaev, L. K. Thompson, *Chem. Soc. Rev.* **2009**, *38*, 2334-2359; e) J. G. Hardy, *Chem. Soc. Rev.* **2013**, *42*, 7881-7899.
- [3] a) J. Hausmann, G. B. Jameson, S. Brooker, *Chem. Commun.* **2003**, 2992-2993; b) J. Hausmann, S. Brooker, *Chem. Commun.* **2004**, 1530-1531; c) J. Klingele (née Hausmann), J. F. Boas, J. R. Pilbrow, B. Moubarak, K. S. Murray, K. J. Berry, K. A. Hunter, G. B. Jameson, P. D. W. Boyd, S. Brooker, *Dalton Trans.* **2007**, 633-645 and front cover feature.
- [4] a) T. Bark, M. Duggelli, H. Stoeckli-Evans, A. von Zelewsky, *Angew. Chem. Int. Ed.* **2001**, *40*, 2848-2851; b) W. Meng, T. K. Ronson, J. K. Clegg, J. R. Nitschke, *Angew. Chem., Int. Ed.* **2013**, *52*, 1017-1021.
- [5] a) A.-M. Stadler, F. Puntoriero, S. Campagna, N. Kyritsakas, R. Welter, J.-M. Lehn, *Chem. Eur. J.* **2005**, *11*, 3997-4009; b) A.-M. Stadler, F. Puntoriero, F. Nastasi, S. Campagna, J.-M. Lehn, *Chem. Eur. J.* **2010**, *16*, 5645-5660; c) A.-M. Stadler, J. Ramirez, J.-M. Lehn, *Chem. Eur. J.* **2010**, *16*, 5369-5378; d) A.-M. Stadler, L. Karmazin, C. Bailly, *Angew. Chem. Int. Ed.* **2015**, *54*, 14570-14574; e) J. Ramirez, A.-M. Stadler, G. Rogez, M. Drillon, J.-M. Lehn, *Inorg. Chem.* **2009**, *48*, 2456-2463.
- [6] a) V. V. Kastron, I. G. Iovel, I. P. Skrastyn'sh, Y. S. Gol'dberg, M. V. Shimanskaya, G. Y. Dubur, *Chemistry of Heterocyclic Compounds* **1986**, *22*, 915-917; b) I. G. Iovel, I. Jansone, Y. S. Gol'dberg, M. V. Shimanskaya, *Khim. Geterotsikl.* **1990**, *4*, 532-537; c) R. Franke, *Ber. Deutsch. Chem. Ges.* **1905**, *38*, 3724-3728; d) M. Hasegawa, Y. Asusuki, F. Susuki, H. Nakanishi, *J. Polym. Sci., Part A: Polym. Chem.* **1969**, *7*,

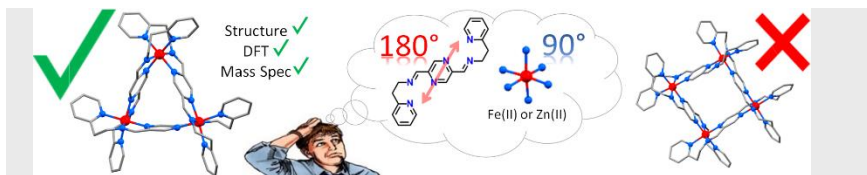
FULL PAPER

- 743-752; e) R. H. Wiley, *Journal of Macromolecular Science: Part A - Chemistry* **1987**, *24*, 1183-1190; f) R. Coufal, M. Prusková, I. Císařová, D. Drahoňovský, J. Vohlídal, *Synth. Commun.* **2016**, *46*, 348-354; g) S. K. Das, J. Frey, *Tetrahedron Lett.* **2012**, *53*, 3869-3872; h) H. A. Staab, W. K. Appel, *Liebigs Ann. Chem.* **1981**, 1065-1072.
- [7] Y. Xiao-Yan, M. Masahiko, K. Mitsuru, K. Susumu, J. Guo-Xin, *Chem. Lett.* **2001**, *30*, 168-169.
- [8] M. Schweiger, S. R. Seidel, A. M. Arif, P. J. Stang, *Angew. Chem. Int. Ed.* **2001**, *40*, 3467-3469.
- [9] S. Derossi, M. Casanova, E. Iengo, E. Zangrando, M. Stener, E. Alessio, *Inorg. Chem.* **2007**, *46*, 11243-11253.
- [10] A. Neels, H. Stoeckli-Evans, *Inorg. Chem.* **1999**, *38*, 6164-6170.
- [11] D. S. Cati, J. Ribas, J. Ribas-Arino, H. Stoeckli-Evans, *Inorg. Chem.* **2004**, *43*, 1021-1030.
- [12] a) J. P. Perdew, W. Yue, *Phys. Rev. B* **1986**, *33*, 8800-8802; b) J. P. Perdew, *Phys. Rev. B* **1986**, *33*, 8822-8824; c) A. D. Becke, *Phys. Rev. A* **1988**, *38*, 3098-3100.
- [13] a) M. Bühl, H. Kabrede, *J. Chem. Theory Comput.* **2006**, *2*, 1282-1290; b) L. J. Kershaw Cook, R. Kulmaczewski, R. Mohammed, S. Dudley, S. A. Barrett, M. A. Little, R. J. Deeth, M. A. Halcrow, *Angew. Chem. Int. Ed.* **2016**, *55*, 4327-4331.
- [14] A. Schäfer, H. Horn, R. Ahlrichs, *J. Chem. Phys.* **1992**, *97*, 2571-2577.
- [15] T. Bark, A. von Zelewsky, D. Rappoport, M. Neuburger, S. Schaffner, J. Lacour, J. Jodry, *Chem. Eur. J.* **2004**, *10*, 4839-4845.
- [16] a) M. Fujita, O. Sasaki, T. Mitsunashi, T. Fujita, J. Yazaki, K. Yamaguchi, K. Ogura, *Chem. Commun.* **1996**, 1535-1536; b) M. Scherer, D. L. Caulder, D. W. Johnson, K. N. Raymond, *Angew. Chem., Int. Ed. Engl.* **1999**, *38*, 1587-1592; c) P. N. W. Baxter, J.-M. Lehn, G. Baum, D. Fenske, *Chem. Eur. J.* **2000**, *6*, 4510-4517; d) F. A. Cotton, C. A. Murillo, R. Yu, *Dalton Trans.* **2006**, 3900-3905.
- [17] a) C. Tanford, *Science* **1978**, *200*, 1012-1018; b) W. Cullen, C. A. Hunter, M. D. Ward, *Inorg. Chem.* **2015**, *54*, 2626-2637.
- [18] O. Mamula, F. J. Monlien, A. Porquet, G. Hopfgartner, A. E. Merbach, A. von Zelewsky, *Chem. Eur. J.* **2001**, *7*, 533-539.
- [19] a) R. H. Blessing, *Acta Crystallogr., Sect. A: Found. Crystallogr.* **1995**, *51*, 33-38; b) G. M. Sheldrick, Göttingen, **1996**.
- [20] G. Sheldrick, *Acta Crystallographica, Section C* **2015**, *71*, 3-8.
- [21] P. van der Sluis, A. L. Spek, *Acta Crystallogr., Sect. A: Found. Crystallogr.* **1990**, *A46*, 194-201.
- [22] C. F. Macrae, I. J. Bruno, J. A. Chisholm, P. R. Edgington, P. McCabe, E. Pidcock, L. Rodriguez-Monge, R. Taylor, J. van de Streek, P. A. Wood, *J. Appl. Crystallogr.* **2008**, *41*, 466-470.
- [23] POVray, Persistence of Vision Raytracer (Version 3.6) ed., Persistence of Vision Raytracer (Version 3.6), **2004**.
- [24] F. Neese, *WIREs Comput. Mol. Sci.* **2012**, *2*, 73-78.
- [25] F. Neese, *J. Comput. Chem.* **2003**, *24*, 1740-1747.
- [26] a) K. Eichkorn, O. Treutler, H. Öhm, M. Häser, R. Ahlrichs, *Chem. Phys. Lett.* **1995**, *240*, 283-290; b) K. Eichkorn, O. Treutler, H. Öhm, M. Häser, R. Ahlrichs, *Chem. Phys. Lett.* **1995**, *242*, 652-660; c) K. Eichkorn, F. Weigend, O. Treutler, R. Ahlrichs, *Theor. Chem. Acc.* **1997**, *97*, 119-124.
- [27] a) A. Klamt, G. Schüürmann, *J. Chem. Soc., Perkin Trans. 2* **1993**, 799-805; b) A. Klamt, *J. Phys. Chem.* **1995**, *99*, 2224-2235; c) A. Klamt, V. Jonas, *J. Chem. Phys.* **1996**, *105*, 9972-9981.
- [28] A. V. Marenich, C. J. Cramer, D. G. Truhlar, *The Journal of Physical Chemistry B* **2009**, *113*, 6378-6396.

FULL PAPER

Layout 2:

FULL PAPER



Ross W. Hogue, Sebastien Dhers, Ryan M. Hellyer, Jingwei Luo, Garry S. Hanan, David S. Larsen, Anna L. Garden* and Sally Brooker*

Page No. – Page No.

Self-Assembly of Cyclohelicate [M₃L₃] Triangles over [M₄L₄] Squares, despite near Linear bis-terdentate L and Octahedral M

Rare cyclohelicate triangle architectures, not *squares* as seen for the bis-terdentate *di-amide* ligand, self-assemble when the *di-imine* analogue is employed. In the triangles, the octahedral metal ions are located 0.4-0.5 Å out of the plane of the bridging pyrazine rings, towards the centre of the triangle. DFT calculations correctly predict the observed triangle architectures to be energetically favoured.